



HAL
open science

Uncertainty Analysis of Spherical Near Field Antenna Measurement System at VHF

Gwenn Le Fur, Francisco Cano-Facila, Luc Duchesne, Daniel Belot, Lise Feat, Anthony Bellion, Kevin Elis, Romain Contreres

► **To cite this version:**

Gwenn Le Fur, Francisco Cano-Facila, Luc Duchesne, Daniel Belot, Lise Feat, et al.. Uncertainty Analysis of Spherical Near Field Antenna Measurement System at VHF. Antenna Measurement Techniques Association; AMTA, Oct 2014, Tucson, United States. hal-01253521

HAL Id: hal-01253521

<https://hal.science/hal-01253521>

Submitted on 11 Jan 2016

HAL is a multi-disciplinary open access archive for the deposit and dissemination of scientific research documents, whether they are published or not. The documents may come from teaching and research institutions in France or abroad, or from public or private research centers.

L'archive ouverte pluridisciplinaire **HAL**, est destinée au dépôt et à la diffusion de documents scientifiques de niveau recherche, publiés ou non, émanant des établissements d'enseignement et de recherche français ou étrangers, des laboratoires publics ou privés.



Distributed under a Creative Commons Attribution 4.0 International License

Uncertainty Analysis of Spherical Near Field Antenna Measurement System at VHF

Gwenn Le Fur, Francisco Cano-Facila,
Luc Duchesne
R&D Department
MVG - SATIMO Industries
Villebon-sur-Yvette, France
Gwenn.le-fur@satimo.fr

Daniel Belot, Lise Feat, Anthony Bellion,
Kevin Elis, Romain Contreres
DCT/RF/AN
CNES (French National Space Center)
Toulouse, France
Daniel.belot@cnes.fr

Abstract— This paper presents parts of investigations done in a VHF spherical Near-Field system in order to estimate measurement uncertainties. First is briefly presented the mono-probe Near-Field system and uncertainties estimations challenges due to low frequencies. Then are described the specific and appropriated approaches for the considered errors terms. Classical pattern comparison is used. Finally is provided a global budget error with and without time filtering to appreciate the benefit of such an approach.

I. INTRODUCTION

Recent needs for monitoring and tracking in low VHF range below 100 MHz imply the use of specific antenna measurement facilities to characterize either the antenna alone or the antenna mounted on a supporting structure which can be heavy and bulky. Conventional outdoor Far-Field antenna measurement ranges used at UHF frequency bands and above become poorly effective down in VHF frequency band due to ground effects and electromagnetic pollution. Other implementations such as indoor Far-Field or compact range are not suitable at these very large wavelengths. The indoor Near-Field approach shows benefits in terms of compactness. However this approach involves issues due to high levels of reflectivity of the anechoic chamber and system components at these frequencies. Studies and characterizations of each component effect have been performed [1] and post processing techniques have been used and compared previously [2] to assess the system performances.

The present paper focuses on measurement uncertainties estimation to qualify the CNES VHF Near-Field system. Based on the well-known 18-NIST terms [3] specific and appropriated approaches of estimation had to be found regarding the present perturbations in the chamber. These approaches are detailed for the main impacting considered terms. To build the budget error two main cases are taken; the unfiltered measurement results and the time domain filtered ones. Not all the error terms are estimated in this paper due to current lack of measurement. Full budget error could be provided for the conference. Thus this paper aims present the approaches of error terms estimation to finally appreciate performances of the low frequencies Near-Field system dealing with the present reflections. The paper is organized as follow; first are described the system, the approaches and the tools used for error estimations. Then are detailed the estimation for

five main terms. Finally are provided two budgets error with and without time-filtering

II. SYSTEM DETAILS AND APPROACHES USED FOR ERROR ESTIMATION

Uncertainties estimation can be performed either for a system (independent of the used antenna under test) or for a specific antenna within a system. In this paper we are in the second case and focus on uncertainty budget of the CNES Near-Field system for a particular Antenna Under Test (AUT).

A. CNES VHF Near-Field Facility

The measurement used is the single probe spherical Near-Field measurement system located in the chamber of the CNES in Toulouse France. This facility is dedicated to perform antenna measurement from 80 MHz to 200 GHz [4]. The chamber is shared by a compact range measurement system and a single probe Near-Field system. Above 400 MHz the compact range configuration is used. Below 400 MHz the Near-Field configuration is used. Nevertheless classical foam pyramidal absorbers are poorly efficient below 200 MHz. Therefore ripples due to reflections coming from the compact range reflector and from the chamber walls are present. In order to extend the operational measurement bandwidth down 100 MHz a new wide band and dual polarized VHF probe has been designed and manufactured [2] (*cf.* Figure 1). All the measurement results presented in this paper have been done by using this probe.



Figure 1 Photograph of the dual polarized probe in the CNES VHF Near-Field system

B. Antenna Pattern Comparison Approach

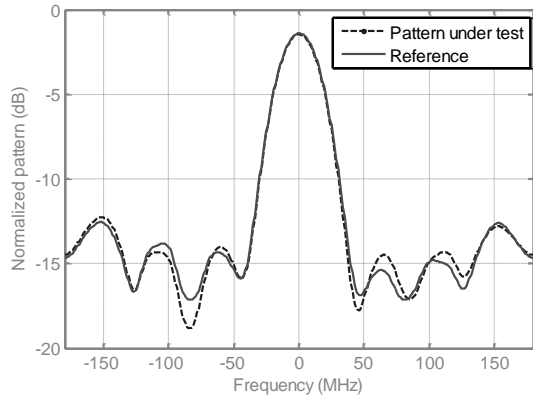
The chosen alternative to estimate some of the error terms later presented in section III is the classical approach based on comparing two different patterns, one of them considered as reference. This strategy was already employed in [5] where four different comparison approaches were presented in order to determine the accuracy of different measurement facilities. In our particular case, it was seen that the most appropriate comparison was the weighted logarithmic difference which is able to de-emphasize the noise and the large spikes. The weighted function W_{log} is composed by the noise function, $W_{n,3}$, and the pattern weighting function, W_p with $\beta = 0.3$ (see [5] for more details). Thus the weighted logarithmic difference between two patterns $f_1(\theta, \varphi)$ and $f_2(\theta, \varphi)$ can be expressed as:

$$\Delta_{w,log}(\theta, \varphi) = W_{log}\Delta_{log}(\theta, \varphi) \quad (1)$$

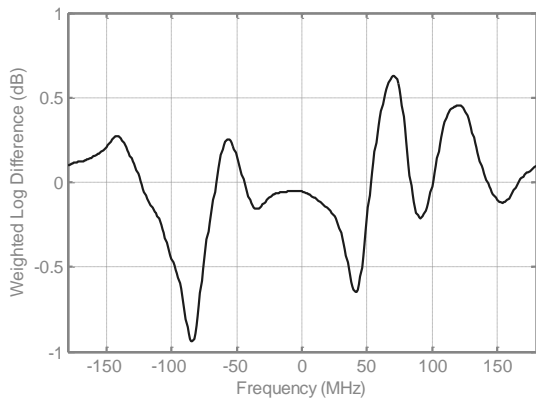
with

$$\Delta_{log}(\theta, \varphi) = 20 \log_{10}f_1(\theta, \varphi) - 20 \log_{10}f_2(\theta, \varphi) \quad (2)$$

Once the difference has been computed, the mean and standard deviation can be calculated in a usual way. These two factors will be used as figures of merit to quantify the difference between the two patterns.



(a)



(b)

Figure 2 Example of patterns comparison (a) and corresponding weighted logarithmic difference (b)

C. CNES Near-Field Coordinate system

The Near-Field coordinate system is as shown in the Figure 3 below where the acquisition on the full sphere is achieved by rotating the AUT around two axes corresponding to the azimuth (φ) and elevation (θ) of the measurement sphere.

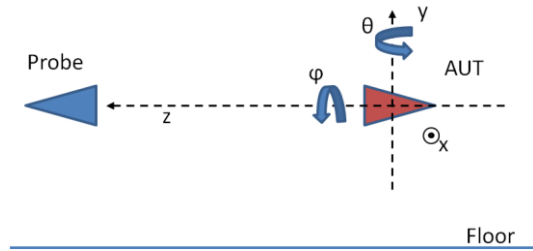


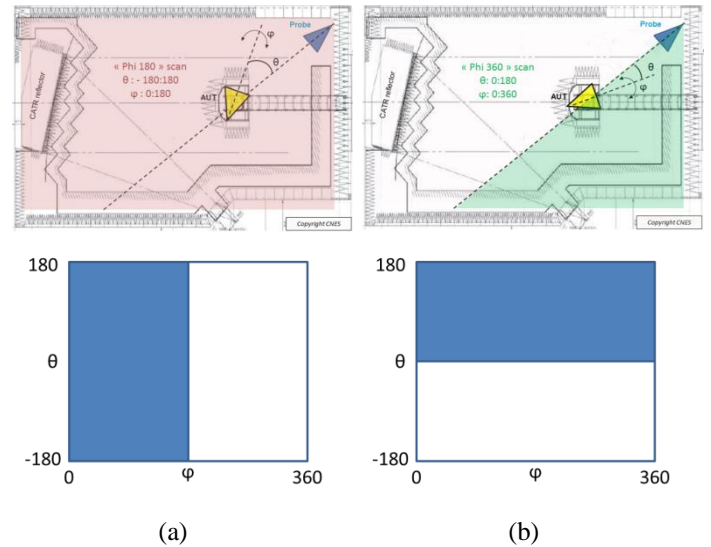
Figure 3 CNES Near-Field coordinate system

D. Scan configurations

As commented in the previous point, the AUT is rotated around two axes to perform the full sphere scan. Because a complete rotation of 360 degrees is possible around both axes, there are two different ways of scanning the full sphere [6]:

- The "180 Phi" scan : $\theta \in [-180; 180]^\circ$ and $\varphi \in [0; 180]^\circ$
- The "360 Phi" scan : $\theta \in [0; 180]^\circ$ and $\varphi \in [0; 360]^\circ$

The "180 Phi" and "360 Phi" areas "seen" by the AUT are illustrated in the Figure 4-a and Figure 4-b, respectively. Due to the theta excursion, the "360 Phi" scan is expected to show more symmetric results than the "180 Phi" scan. Indeed in this last case perturbations coming from the CATR reflector are stronger than the ones coming from the opposite wall. Due to this fact, the "360 Phi" scan with time domain filtering (described in the next point) is taken as reference in the comparisons (this fact has been also validated by comparing with simulations, providing the "360 Phi" scan better results).



(a)

(b)

Figure 4 Illustration of the "180 phi" scan (a) and "360 phi" scan (b) configuration

E. Time Domain Filtering Approach

Because the measurements are performed at VHF, as commented later, the main source of error are reflections coming from the walls of the chambers. Although the chamber is covered with absorbent material, the reflectivity of such a material at these frequencies is not so big. Due to this reason, a filtering in the time domain is applied in order to reduce the unwanted contributions. This filtering is a classical approach [7] and it is based on measuring over a wide enough frequency range. Using these data, the time response is immediately calculated by applying an inverse Fourier transform. If there are contributions coming from different places in the measurement set-up (different distances and therefore different times of arrival), it is very simple to identify them in this new domain. After that, direct contribution is detected and gated, eliminating the delayed response due to the reflected and diffracted components. Finally, a Fourier transform is applied to return to the frequency-domain.

III. ERRORS TERMS ESTIMATION

A. Probe alignment

This error appears when the probe is not well aligned with the measurement axis. To estimate the error due to this misalignment, we consider polar patterns obtained through the calibration measurement (360° phi scan on-axis). Once applied calibration coefficients on this calibration measurement result, we note the differences between 90° spaced values which relies the probe capability to discriminate cross-polarization level. As the angular sampling for this measurement is 1° we record the differences at $\pm 0.5^\circ$ (the maximum error of alignment which could be committed for this given angular sampling step). Thus we obtain a error value which will be involved in the cross-polarization error budget. The variation of this error value versus frequency is shown in Figure 5.

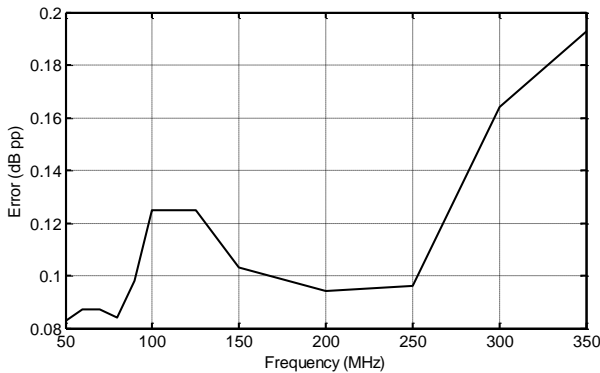


Figure 5 STD values of probe alignment error versus frequency

B. Probe y position errors

To estimate the probe y-position error an additional measurement with a 2 cm offset in the y-direction was performed. The results of this measurement were compared in Far-Field with the ones obtained in the assumed good y-location of the probe. The pattern comparison approach described in section II.B is applied and the variation of this

error value versus frequency is shown in Figure 6 for both Co and Cross-polarization.

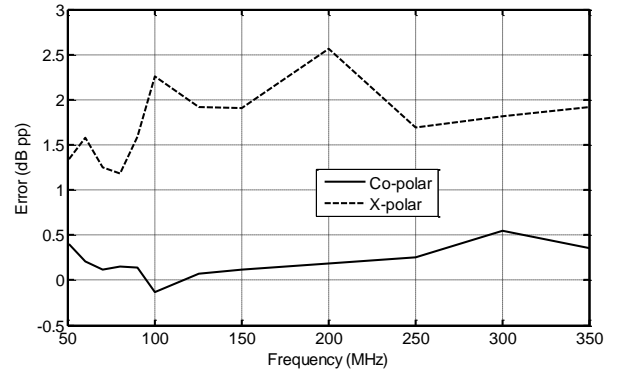


Figure 6 STD values of probe y-position error versus frequency

C. Probe z position errors

This error appears when the distance from the center of rotation of the AUT to the phase center of the probe is different to that one considered in the Near-Field to Far-Field transformation process. If the phase center of the probe is well-known, this error is negligible. However, the phase center could change in a great way in frequency, especially in low frequency. Therefore, when measuring in a very large frequency range because the measurement distance is considered constant for all the frequency points, there will not be a negligible z-position error. In fact, this is the situation in our measurement. The Near-Field distance is considered to be equal to 4.4 m. However, the phase center position of our probe is different depending on the frequency.

One method to estimate the impact of this error is to compute and compare the Far-Field patterns assuming that the acquisition has been performed over a sphere of 4.4 m radius and $4.4 + \Delta z$ m radius. Δz is considered to be equal to the maximum variation of the phase center (around 0.8 m, value which has been calculated both from simulations and measurements). The impact of an error of 0.8 m (worst case) in the z-position of the probe introduces the Far-Field errors depicted in the following figure.

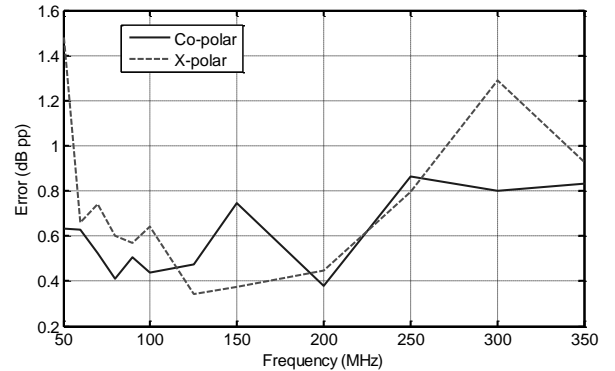


Figure 7 STD values of probe z-position error versus frequency

Logically, this error can be avoided by using for each frequency the appropriate Near-Field distance and for that, the phase center positions of the probe as a function of the frequency must be known.

D. Room scattering

Usual approach to estimate the room scattering impact consists in moving the whole measurement system in the chamber by $\lambda/4$ steps. For each system location is measured the whole antenna pattern. Such an approach is not implementable in our case considering the wavelengths and the system setup. Consequently we propose here to use the available “180 Phi” and “360 Phi” measurement results of the same antenna to estimate the room scattering effect. “360 Phi” scan results with time filtering are taken as reference. To this reference are compared the “180 Phi” scan results with and without time filtering. Results versus frequency for Co and Cross polarization are presented in Figure 8. We can clearly appreciate through this plot the benefit of the time filtering for this particular AUT.

In this contribution is assumed to be included the “Multiple Reflections” term between probe and antenna under test.

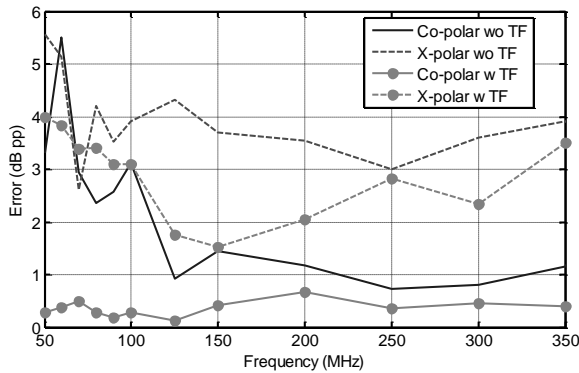


Figure 8 STD values of probe room scattering error versus frequency

E. Random errors

A two-step method is employed to determine the impact of random errors in Far-Field results. The first step is based on estimating the noise power in the current Near-Field data. For that purpose, the spherical wave coefficients obtained from simulated Near-Field noise with different power levels are compared with the spherical wave coefficients calculated from the acquired Near-Field data. As observed in Figure 9, the lower order modes contain the information about the AUT and after a given value modes only have information about the noise. Therefore, by comparing the higher order modes of the spherical expansions commented before it is possible to determine the noise power present in the Near-Field data. In our system, for example, the noise power is 43 dB below the maximum, that is, the signal-to-noise ratio in Near-Field is 43 dB.

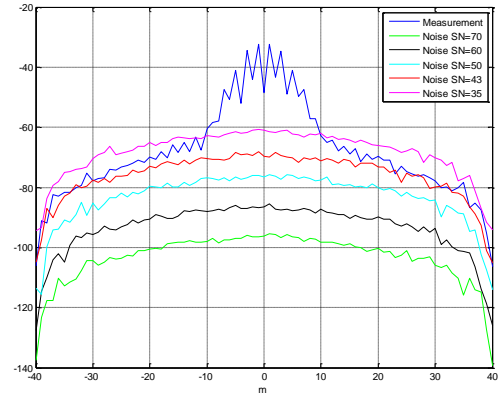


Figure 9 Modal contents of the measurement and several noise powers

Once the noise power is known in Near-Field (determined spherical wave spectrum analysis), it is possible to assess the behavior of such a noise in Far-Field by simply using Montecarlo method. This method typically runs simulations many times over in order to obtain the distribution of an unknown probabilistic entity. Logically, the larger the number of simulations is, the better the estimation of the random variable is. In our particular case, we want to determine the properties of the Far-Field noise due to a known Near-Field noise. This is achieved by following the next steps:

- A reference Far-Field pattern is computed by using Near-Field data.
- Near-field data is corrupted by adding a noise with the power level determined in the first stage and the corresponding corrupted Far-Field pattern is computed.
- Then, the reference and corrupted Far-Field patterns are compared, obtaining the error pattern (noise in Far-Field).
- The two previous steps are repeated several times in order to obtain a better estimation of the properties of the noise in Far-Field.
- Finally, all the error patterns are used to determine the mean and the standard deviation of the Far-Field noise.

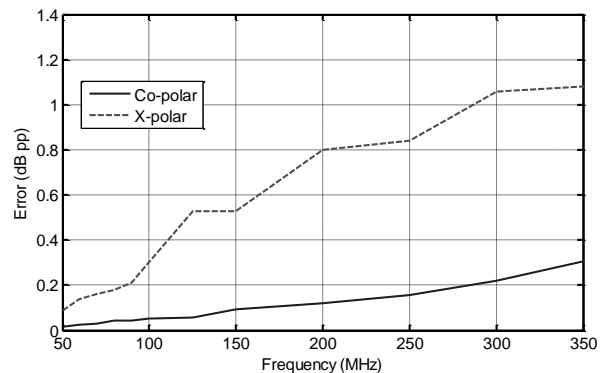


Figure 10 STD values of random error versus frequency

IV. RESULTS

Tables I and II present the budgets error for the unfiltered and the time-filtered cases respectively. For each frequency point are provided the mean and the standard deviation for the Co and the Cross polarization results. These power budget rely measurement uncertainties by considering the contribution of the five error terms previously analyzed.

TABLE I. BUDGET ERROR WITHOUT TIME FILTERING.

Frequency (MHz)	Co-Pol		X-Pol	
	μ (dB)	STD (dBpp)	μ (dB)	STD (dBpp)
50	-1.3	3.4	1.8	5.9
60	-4.0	5.5	3.8	5.4
70	-1.9	3.0	3.0	3.0
80	-0.6	2.4	1.5	4.4
90	-0.3	2.6	3.2	3.9
100	-1.2	3.1	1.8	4.6
125	-0.5	1.0	0.3	4.8
150	-0.7	1.6	0.1	4.2
200	-0.1	1.3	1.2	4.5
250	-0.5	1.2	0.3	3.6
300	-0.4	1.3	0.2	4.4
350	-0.5	1.5	1.5	4.6

TABLE II. BUDGET ERROR WITH TIME FILTERING.

Frequency (MHz)	Co-Pol		X-Pol	
	μ (dB)	STD (dBpp)	μ (dB)	STD (dBpp)
50	-0.1	0.8	0.9	4.5
60	-0.1	0.8	0.4	4.2
70	-0.3	0.7	-0.3	3.7
80	-0.1	0.5	-0.1	3.7
90	-0.2	0.6	-0.3	3.5
100	-0.3	0.5	-0.9	3.9
125	-0.1	0.5	0.1	2.7
150	-0.4	0.9	-0.8	2.5
200	-0.2	0.8	-0.2	3.4
250	-0.2	1.0	-0.1	3.5
300	0.0	1.1	0.5	3.4
350	-0.5	1.0	0.6	4.3

We globally observe the expected improvement by applying time-filtering. This observation comes from two main reasons; firstly the room scattering error is one of the bigger impacts at low frequency and time domain filtering aims to reduce this impact. Secondly the reference measurement result

used in pattern comparison for the estimation of several terms is time filtered to be closer to simulation results.

Another observation at high frequency is the fact that we retrieve the behavior of the noise contribution in both error budgets. This is partly due to the absence of time-filtering in the random error term estimation.

V. CONCLUSION AND PROSPECTS

Through investigations done in the CNES VHF spherical Near-Field system this paper provides a partial estimation of measurement uncertainties. First was presented the mono-probe near field system and uncertainties estimations challenges due to low frequencies. Specific and appropriated approaches for the estimation of five considered errors terms are detailed. Finally was provided a global budget error with and without time filtering to appreciate the benefit of such an approach.

This study provides a first estimation of the system measurement uncertainties for one particular antenna under test. Ongoing works aim to build a full system error budget independent of the measured antenna.

REFERENCES

- [1] Le Fur, G.; Duchesne, L.; Durand, L.; Bellion, A.; Belot, D., "Feasibility of indoor spherical near field antenna measurement facility in VHF range", Antenna Technology and Applied Electromagnetics (ANTEM), 2012 15th International Symposium on, pp.1-7, 25-28 June 2012.
- [2] Le Fur, G.; Cano-Facila F.; Saccardi F.; Belot, D.; Durand L.; Duchesne L.; Foged L.; Lopez J-M.; Bellion, A. "Improvement of Antenna Measurement Results at Low Frequencies by Using Post-processing Techniques", EuCAP 2014 8th International Symposium on ,The Hague, The Netherlands.
- [3] Newell, AC., "Error analysis techniques for planar near-field measurements," Antennas and Propagation, IEEE Transactions on , vol.36, no.6, pp.754,768, Jun 1988
- [4] GDR Ondes "Rapport sur le recensement des chambres anéchoïques française et leurs perspectives » 2010
- [5] Pivnenko, S.; Pallesen, J.E.; Breinbjerg, O.; Castaner, M.S.; Almena, P.C.; Portas, C.M.; Sanmartin, J.L.B.; Romeu, J.; Blanch, S.; Gonzalez-Arbesu, J.M.; Sabatier, C.; Calderone, A; Portier, G.; Eriksson, H.; Zackrisson, J., "Comparison of Antenna Measurement Facilities With the DTU-ESA 12 GHz Validation Standard Antenna Within the EU Antenna Centre of Excellence," Antennas and Propagation, IEEE Transactions on , vol.57, no.7, pp.1863-1878, July 2009
- [6] G.E. Hindman and A.C. Newell, "Spherical near-field self-comparison measurements," in 26th AMTA Annual Meeting & Symposium, Atlanta, Ga, USA, October 2004
- [7] S. Loredó, M. R. Pino, F. Las-Heras, and T. K. Sarkar, "Echo identification and cancellation techniques for antenna measurement in non-anechoic test sites," *IEEE Antennas Propagat. Mag.*, vol. 46, No. 1, pp. 100-107, Feb., 2004.